Chain entanglement and melt viscosity of compatible polymer blends: poly(methyl methacrylate) and poly(styrene–acrylonitrile)

Souheng Wu

E. I. du Pont de Nemours & Company, Central Research and Development Department, Experimental Station, Wilmington, Delaware 19898, USA

(Received 5 May 1986; revised 25 August 1986; accepted 14 October 1986)

The plateau modulus and zero-shear melt viscosity of binary compatible blends of poly(methyl methacrylate) and an azeotropic poly(styrene–acrylonitrile) were measured by dynamic oscillation and shear creep, and used to analyse the entanglement behaviour between dissimilar chains and the compositional dependence of zero-shear melt viscosity. It is found that, due to specific interchain interactions (which give rise to the molecular miscibility), dissimilar chains are less likely to entangle than similar chains. The zero-shear melt viscosity η_0 obeys the simple relation, $\log \eta_0 = \phi_1 \log \eta_{01} + \phi_2 \log \eta_{02}$, where ϕ is the volume fraction, and the subscripts 1 and 2 refer to the two pure components, respectively, for the present blends.

(Keywords: chain entanglement; melt viscosity; density; glass transition temperature; compatible polymer blends; poly(methyl methacrylate); poly(styrene–acrylonitrile)

INTRODUCTION

Chain entanglement is an important factor in the rheological[1,2], mechanical[3,4] and adhesive[5,6] properties of polymers. In this work, we study the entanglement between dissimilar compatible chains: poly(methyl methacrylate) and azeotropic poly(styrene–acrylonitrile). Such studies are relevant to the understanding of the effects of molecular structure and specific interchain interactions on entanglement behaviour.

EXPERIMENTAL

A poly(methyl methacrylate) (PMMA, component 1) and a poly(styrene–acrylonitrile) (SAN, component 2) were used as the two pure components. The SAN is an azeotropic copolymer, having $74.9 \pm 0.1\%$ by weight of styrene, and $24.1 \pm 0.2\%$ by weight of acrylonitrile, determined by elemental analysis, which is the azeotropic composition[7].

The molecular weights were determined by gel permeation chromatography with tetrahydrofuran as the solvent, using pure standards calibrated by light scattering and osmometry. The weight-average molecular weight M_w and the number-average molecular weight M_n are, respectively, 120 000 and 48 700 for the PMMA, and 220 000 and 112 000 for the SAN. The M_w and M_n for the blends were calculated by

$$M_w = w_1 M_{w1} + w_2 M_{w2}$$

and

$$1/M_n = w_1/M_{n1} + w_2/M_{n2}$$

where w is the weight fraction, and the subscripts 1 and 2 refer to the components 1 and 2, respectively.

Preparation of blends

Binary blends of PMMA and SAN of various compositional ratios were prepared by melt extrusion at 200°C melt temperature. It is important to ensure that the polymers were not thermomechanically degraded during the extrusion. To verify this, pure PMMA and SAN were also individually extruded under the same conditions as for the blends. Their zero-shear melt viscosities and the intrinsic viscosities in tetrahydrofuran were measured and found to be unchanged before and after the extrusion, confirming that the polymers were not degraded during the extrusion. On the other hand, we found that extrusion above 230°C (i.e. the ceiling temperature of PMMA) would result in considerable degradation.

Freeze-drying from a solution was advocated as a preferred method for preparing some compatible blends[8]. However, we found that PMMA/SAN blends freeze-dried from benzene solutions gave hazy films, because of phase separation during the process due to solvent effects. On the other hand, those blends freeze-dried from mixtures of benzene and tetrahydrofuran were clear and have the same rheological properties as those prepared by melt extrusion. This shows that proper solvents must be used in the freeze-drying method to avoid solvent effects, and that the present melt-extruded blends are identical to properly freeze-dried blends.

Compatibility, glass transition and density

PMMA and SAN (with 9 to 30% by weight of acrylonitrile) have been shown to be molecularly compatible by T_g measurements[9,10], electron microscopy[9,11], small-angle neutron scattering[12–14], pulsed n.m.r.[15] and cloud point measurements[14,16–18]. When the SAN contains less than 28% by weight of acrylonitrile, PMMA/SAN blends show a single lower-consolute curve. However, even a minute increase of

0032-3861/87/071144/05$03.00

acrylonitrile content above 28% by weight in the SAN will split the single lower-consolute curve into two curves with an added upper-consolute curve. This was found by Schmitt and coworkers[14,16] and successfully interpreted in terms of the behaviour of χ parameter by Koningsveld and coworkers[19]. Therefore, an azeotropic SAN with $24.1 \pm 0.2\%$ by weight of acrylonitrile is used in this work to ensure its compositional uniformity and a simple phase behaviour.

The cloud points for all the blends were measured to confirm that the present blends have a single lower-consolute curve. The cloud points were reproducible within ± 1°C. The lower critical solution temperature (*LCST*) was found to be 236 ± 1°C.

The T_g values were determined by d.s.c., reproducible within ± 0.5°C. Only a single intermediate T_g was found for each blend. *Figure 1* plots the T_g *versus* composition, showing a positive deviation from linearity, consistent with the literature[9,10].

The melt density was measured dilatometrically at 180°C, given by

$$v = 0.9132 w_1 + 1.021 w_2 \quad (1)$$

where v is the specific volume ($cm^3\ g^{-1}$) at 180°C, accurate within $\pm 0.05\%$.

The χ parameter for PMMA/SAN blends has been reported to be -0.011, determined by small-angle neutron scattering[12-14,20]. The SAN copolymer coil in the blend was found to be slightly expanded over that in the θ condition; its root-mean-square end-to-end distance R varies with the molecular weight as $R \propto M^{0.6}$, showing compatibility of PMMA and SAN on the molecular scale.

Rheological measurements

All rheological measurements were made below 200°C, i.e. far below the *LCST* and the degradation ceiling temperature, to ensure that the blends were in the compatible region and thermally stable.

The melt viscosity was measured by shear creep at 180°C with a cone and plate at constant stresses of 10^2 to 10^4 dyn cm^{-2} in a Rheometrics Stress Rheometer. The melt viscosity reached the Newtonian region below a shear stress of about 10^3 dyn cm^{-2}, corresponding to a shear rate of about $10^{-4}\ s^{-1}$. The zero-shear melt viscosities obtained are accurate with variations less than 5%.

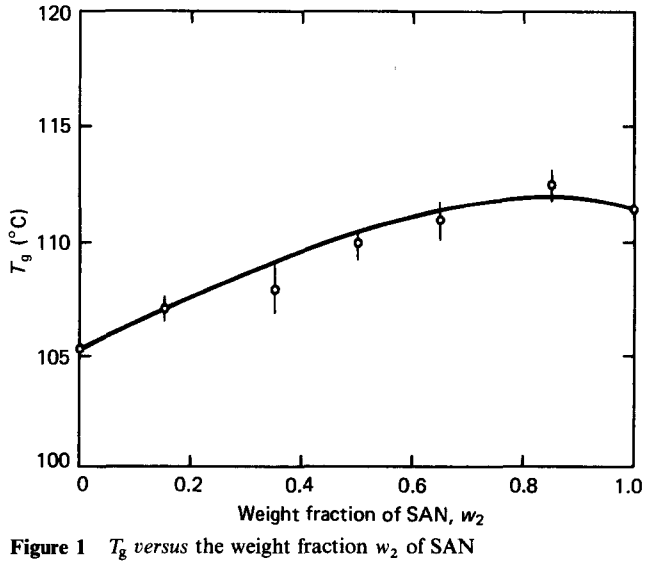

Figure 1 T_g *versus* the weight fraction w_2 of SAN

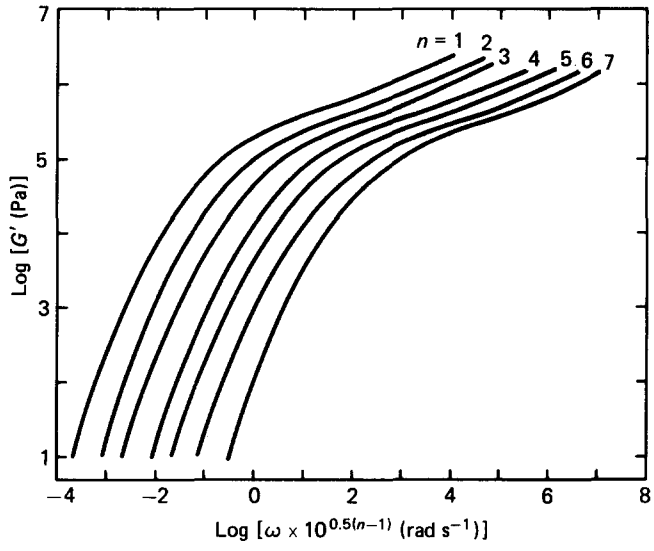

Figure 2 Dynamic storage modulus G' master curves at 160°C. The rate ω is plotted as $\omega \times 10^{0.5(n-1)}$ rad s^{-1}, where n is the curve number, so that the curves are shifted to the right by the designated amount to improve legibility. Curve 1: $n=1$, $w_2=0$; curve 2: $n=2$, $w_2=0.15$; curve 3: $n=3$, $w_2=0.35$; curve 4: $n=4$, $w_2=0.50$; curve 5: $n=5$, $w_2=0.65$; curve 6: $n=6$, $w_2=0.85$; curve 7: $n=7$, $w_2=1.00$

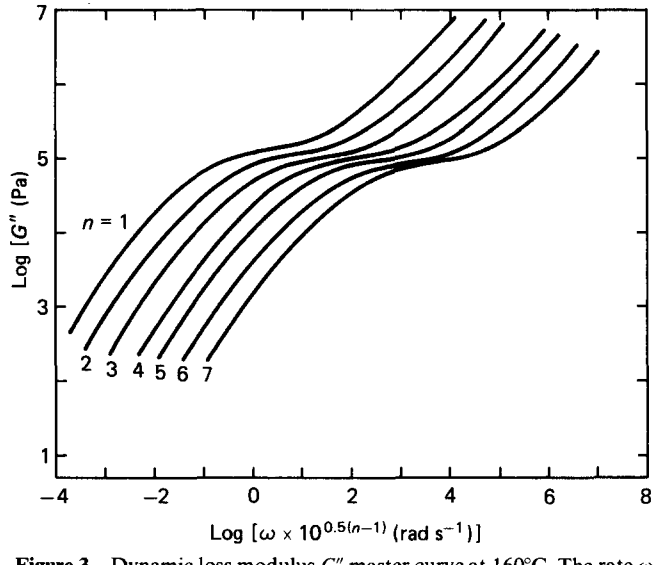

Figure 3 Dynamic loss modulus G'' master curve at 160°C. The rate ω is plotted as $\omega \times 10^{0.5(n-1)}$ rad s^{-1}, where n is the curve number, so that the curves are shifted to the right by the designated amount to improve legibility. Curve 1: $n=1$, $w_2=0$; curve 2: $n=2$, $w_2=0.15$; curve 3: $n=3$, $w_2=0.35$; curve 4: $n=4$, $w_2=0.50$; curve 5: $n=5$, $w_2=0.65$; curve 6: $n=6$, $w_2=0.85$; curve 7: $n=7$, $w_2=1.00$

The linear viscoelastic dynamic moduli spectra were determined by sinusoidal oscillation using a cone and plate between 140 and 200°C in a Rheometrics Mechanical Spectrometer System IV. The curves were superimposed to give master curves at 160°C, shown in *Figures 2* and *3*. A single WLF shift factor a_T was found to be applicable, i.e.

$$\log a_T = 20.67(T - T_g)/(58.33 + T - T_g) \quad (2)$$

where T is the temperature and T_g the glass transition temperature.

The plateau modulus G_N° was determined as the storage modulus G' in the plateau zone at the frequency where $\tan\delta$ was at a minimum. The G_N° values thus obtained

from the master curves were reproducible within 5%. The $(\tan\delta)_{min}$ values were 0.383 to 0.407, depending on the composition.

RESULTS AND DISCUSSION

Analysis of entanglement

Consider pairwise interactions in a binary blend, consisting of volume fractions ϕ_1 and ϕ_2 of components 1 and 2, respectively. There are 1–1, 2–2 and 1–2 type entanglement points. Assume that every contact between two chains i and j has a constant probability of entanglement p_{ij}. In a unit volume of the blend, the number of contacts between two similar chains k is proportional to ϕ_k^2, and that between two dissimilar chains is proportional to $2\phi_1\phi_2$. The total number of entanglement points per unit volume is

$$\rho/M_e = p_{11}\phi_1^2 + p_{22}\phi_2^2 + 2p_{12}\phi_1\phi_2 \quad (3)$$

where ρ is the density of the blend, M_e the average entanglement molecular weight of the blend, $p_{11}=\rho_1/M_{e1}^\circ$, $p_{22}=\rho_2/M_{e2}^\circ$ and $p_{12}=(\rho_1\rho_2)^{1/2}/M_{e12}^\circ$. The M_{e1}° and M_{e2}° are the entanglement molecular weights of pure components 1 and 2, respectively, and M_{e12}° is that of a hypothetical pure component of density $(\rho_1\rho_2)^{1/2}$ having the same entanglement probability as between the dissimilar chains in the blend.

The entanglement molecular weight is related to the density and the plateau modulus by

$$M_e = \rho RT/G_N^\circ \quad (4)$$

Using equation (4) in equation (3) gives

$$G_N^\circ = \phi_1^2 G_{N1}^\circ + \phi_2^2 G_{N2}^\circ + 2\phi_1\phi_2 RT(\rho_1\rho_2)^{1/2}/M_{e12}^\circ \quad (5)$$

which can be transformed to

$$1/M_e = w_1/M_{e1}^\circ + w_2/M_{e2}^\circ - (1-\lambda)(\rho/\rho_1\rho_2)(\rho_1/M_{e1}^\circ + \rho_2/M_{e2}^\circ)w_1w_2 \quad (6)$$

where

$$\lambda = \frac{2(\rho_1\rho_2)^{1/2}/M_{e12}^\circ}{\rho_1/M_{e1}^\circ + \rho_2/M_{e2}^\circ} \quad (7)$$

As shown below, λ is the ratio of entanglement probability between dissimilar chains in the real blend p_{12} to that in a 'reference' blend p_{12}^0. If this model is correct, then λ should be independent of the composition, as indeed shown later.

The reference blend is defined as one in which the total number of entanglement points of all types in a unit volume n° is equal to the sum of those in the two constituent pure components, i.e.

$$n^\circ = \phi_1\rho_1/M_{e1}^\circ + \phi_2\rho_2/M_{e2}^\circ$$

In such a reference blend, the number density of entanglement points between dissimilar chains is

$$n_{12}^\circ = 2p_{12}^\circ\phi_1\phi_2 = \phi_1\phi_2(\rho_1/M_{e1}^\circ + \rho_2/M_{e2}^\circ)$$

where p_{12}° is the entanglement probability between dissimilar chains in the reference blend. Therefore, we have

$$\lambda = p_{12}/p_{12}^\circ \quad (8)$$

Further, it can be shown that the entanglement probability between dissimilar chains in the reference blend is equal to the arithmetic mean of those in the respective pure components, i.e.

$$p_{12}^\circ = \tfrac{1}{2}(p_{11}^\circ + p_{22}^\circ) \quad (9)$$

The present choice of reference blend provides a convenient benchmark for comparing the entanglement behaviour between dissimilar chains in different systems. More importantly, however, the present reference blend is, in fact, the θ blend in which $\chi=0$, as will be shown elsewhere[21].

Plateau modulus

The plateau modulus is plotted *versus* the volume fraction ϕ_2 of SAN in *Figure 4*. The G_N° shows a negative deviation from linearity, indicating that the total number of entanglement points per unit volume in a blend is smaller than the sum of those in the two constituent pure components. Least-squares regression shows that the plot fits equation (5) very well, giving

$$M_{e12}^\circ = 12\,600 \pm 300 \quad (10)$$

Since M_{e1}°(PMMA)=8760 and M_{e2}°(SAN)=11 000, we have M_{e12}° greater than either M_{e1}° or M_{e2}°, indicating that dissimilar chains are less likely to entangle with each other than similar chains.

Entanglement molecular weight

The entanglement molecular weights for pure components and blends are calculated by equation (4) from the plateau modulus. *Figure 4* also plots the $1/M_e$ *versus* the weight fraction w_2 of SAN, showing a negative deviation from linearity. Least-squares regression shows that the plot fits equation (6) very well, giving

$$\lambda = 0.775 \pm 0.005 \quad (11)$$

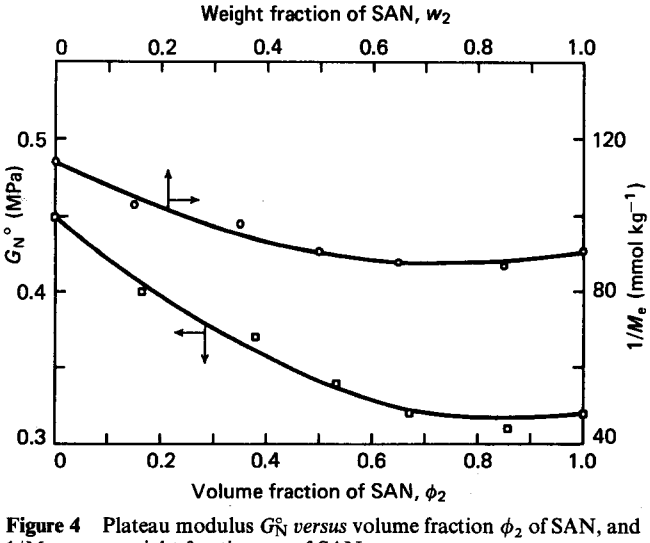

Figure 4 Plateau modulus G_N° *versus* volume fraction ϕ_2 of SAN, and $1/M_e$ *versus* weight fraction w_2 of SAN

which indicates that the probability of entanglement between dissimilar chains in the real blend is smaller than that in the reference blend by a factor of about 1.5.

Zero-shear melt viscosity

The zero-shear melt viscosity η_0 at 180°C for 'as-blended' blends is plotted *versus* w_2 in *Figure 5*, showing a positive deviation from linearity. The molecular weights of the blends are, however, not constant, i.e. increasing with increasing w_2. Thus, the positive deviation may be due to the molecular weight effect. To compare the η_0 at the same molecular weight, we scaled the η_0 to the constant $M_w = 220\,000$ (i.e. the M_w of SAN) by[22]

$$\eta_0(M_w) = (M_w/M_w')^{3.4}\eta_0(M_w') \quad (12)$$

The η_0 at the constant $M_w = 220\,000$ is also plotted in *Figure 5*. A simple linear relation is obtained at constant M_w for the present blends. Since PMMA and SAN have very similar densities, the weight fraction and volume fraction are nearly the same. It is more correct to use the volume fraction, as shown elsewhere[21]; we thus write for the present blends at constant M_w,

$$\log \eta_0 = \phi_1 \log \eta_{01} + \phi_2 \log \eta_{02} \quad (13)$$

where η_{0k} is the zero-shear melt viscosity of pure component k.

Although equation (13) applies very well to PMMA/SAN blends, it is not expected to be generally applicable to other compatible blends. For instance, the melt viscosities of compatible blends of PMMA and poly(vinylidene fluoride)[23], of poly(styrene–maleic anhydride) and poly(styrene-acrylonitrile)[24], of poly(ester carbonate) and poly(ethylene terephthalate)[25] showed negative deviations from linearity. On the other hand, Prest and Porter[8] reported the η_0 for the compatible blends of polystyrene and poly(2,6-dimethyl-1,4-phenylene oxide) (PPO, component 2). The data cover a relatively narrow composition range, $w_2 = 0$ to 0.4. Therefore, it is difficult to determine with certainty if the curve shows any negative or positive deviation from linearity.

The η_0 at a constant molecular weight is affected by chain entanglement, interchain friction and free volume. A complete analysis taking into account all these factors has been made, and will be reported elsewhere[21]. A general equation is thus derived, and shown to reduce to the linear form of equation (13) for the present blends[21].

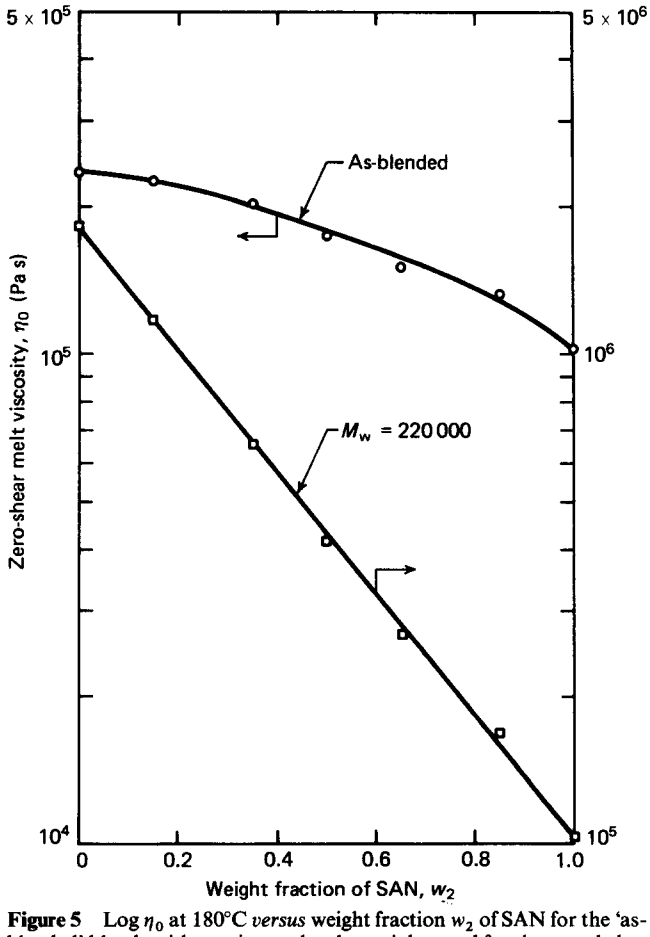

Figure 5 Log η_0 at 180°C *versus* weight fraction w_2 of SAN for the 'as-blended' blends with varying molecular weights, and for those scaled to the constant $M_w = 220\,000$

Effect of interchain interactions

Aharoni[26] has shown that the number of atoms on the main-chain backbone between entanglement points, N_e, is related to the characteristic ratio C_∞ by $N_e \propto C_\infty^2$. This suggests that entanglement is largely controlled by chain convolution. Specific interchain interactions, responsible for molecular compatibility of dissimilar polymers, tend locally to align the chain segments for association and thus stiffen the chains and reduce their convolution, resulting in reduced entanglement between dissimilar chains. Therefore, compatible dissimilar chains are generally less likely to entangle with each other than similar chains. This is supported by the correlation between the χ parameter and the λ value, discussed below.

We have also studied the entanglement behaviour in the compatible blends of PMMA and poly(vinylidene fluoride) (PVF2)[23], and analysed the data of the compatible blends of polystyrene (PS) and poly(2,6-dimethyl-1,4-phenylene oxide) (PPO) reported by Prest and Porter[8] by using our present model[23]. *Table 1* summarizes the χ and λ values for the three systems studied so far. It can be seen that, as the interchain interaction becomes stronger (i.e. more negative χ), the entanglement probability between dissimilar chains becomes smaller (i.e. smaller λ), consistent with our view.

CONCLUSIONS

Specific interchain interactions, responsible for molecular compatibility of dissimilar polymers, tend locally to align the chain segments for association and thus stiffen the chains, and reduce their convolution, resulting in reduced entanglement between dissimilar chains. The stronger the interchain interactions, the smaller the entanglement probability between dissimilar chains.

The zero-shear melt viscosity of PMMA/SAN blends obeys a linear semilogarithmic blending law. However, in

Table 1 Effect of χ parameter on entanglement probability between dissimilar chains λ

Compatible pair	χ	λ
PMMA/PVF2	−0.295[a]	0.309 ± 0.038[d]
PS/PPO	−0.060[b]	0.725 ± 0.013[d]
PMMA/SAN	−0.011[c]	0.775 ± 0.005

[a] Ref. 27; [b] ref. 28; [c] ref. 12; [d] ref. 23

general, deviations from linearity may occur, depending on the nature of entanglement, interchain friction and free volume of the blends.

REFERENCES

1 Ferry, J. D., 'Viscoelastic Properties of Polymers', 3rd Edn., Wiley, New York, 1980
2 Graessley, W. W. *Adv. Polym. Sci.* 1982, **47**, 1
3 Prentice, P. *J. Mater. Sci.* 1985, **20**, 1445
4 Aharoni, S. M. *Macromolecules* 1985, **18**, 2624
5 Wu, S., 'Polymer Interface and Adhesion', Marcel Dekker, New York, 1982
6 Wu, S., Chuang, H. K. and Han, C. D. *J. Polym. Sci., Polym. Phys. Edn.* 1986, **24**, 143
7 Karam, H. J. in 'Polymer Compatibility and Incompatibility', (Ed. K. Solc), Harwood, New York, 1982, pp. 93–106
8 Prest, Jr, W. M. and Porter, R. S. *J. Polym. Sci.* (*A*-2) 1972, **10**, 1639
9 Stein, D. J., Jung, R. H., Illers, K. H. and Hendus, H. *Angew. Makromol. Chem.* 1974, **36**, 89
10 Naito, K., Johnson, G. E., Allara, D. L. and Kwei, T. K. *Macromolecules* 1978, **11**, 1260
11 McMaster, L. P. 'Copolymers, Polyblends and Composites', ACS Adv. Chem. Ser. 142, American Chemical Society, Washington DC, 1975, p. 43
12 Schmitt, B. J., Kirste, R. G. and Jelenic, J. *Makromol. Chem.* 1980, **181**, 1655
13 Kruse, W. K., Kirste, R. G., Haas, J., Schmitt, B. J. and Stein, D. J. *Makromol. Chem.* 1976, **177**, 1145
14 Schmitt, B. J. *Angew. Chem.* (*Int. Engl. Edn.*) 1979, **18**, 273
15 McBrierty, V. J., Douglass, D. C. and Kwei, T. K. *Macromolecules* 1978, **11**, 1265
16 Schmitt, B. J. *Ber. Bunsenges. Phys. Chem.* 1985, **89**, 1133
17 McMaster, L. P. *Macromolecules* 1973, **6**, 760
18 Bernstein, R. E., Cruz, C. A., Paul, D. R. and Barlow, J. W. *Macromolecules* 1977, **10**, 68
19 Koningsveld, R., Kleintjens, L. A. and Leblans-Vinck, A. M. *Ber. Bunsenges. Phys. Chem.* 1985, **89**, 1234
20 Koningsveld, R. and Kleintjens, L. A. *J. Polym. Sci., Polym. Phys. Edn.* 1977, **61**, 221
21 Wu, S., in preparation
22 Friedman, E. M. and Porter, R. S. *Trans. Soc. Rheol.* 1975, **19**, 493
23 Wu, S. *J. Polym. Sci., Polym. Phys. Edn.* 1987, **25**, 557
24 Aoki, K. *Polym. J.* (*Japan*) 1984, **16**, 431
25 Aharoni, S. M. *J. Macromol. Sci.–Phys.* 1983–84, **B22**, 813
26 Aharoni, S. M. *Macromolecules* 1983, **16**, 1722
27 Nishi, T. and Wang, T. T. *Macromolecules* 1975, **8**, 909
28 Maconnachie, A., Kambour, R. P., White, D. M., Rostami, S. and Walsh, D. J. *Macromolecules* 1984, **17**, 2645